Supplementary information

Equilibrium Chain Exchange in Block Copolymer Micelle Solutions by Dissipative Particle Dynamics Simulations

Zhenlong Li, Elena E. Dormidontova

Department of Macromolecular Science and Engineering, Case Western Reserve University, Cleveland, Ohio 44106

1. Estimation of the plateau level for hybridization correlation function I(t).

As discussed in the main paper, the hybridization correlation function I(t) eq.1 reaches a non-zero plateau level at longer times (Figure 2) because of statistical fluctuations in chain distribution among micelles. To estimate the plateau level of I(t), we performed the following calculations. In our simulations, each chain is numbered consequently, for example, for A_2B_3 micelle solution at φ = 0.05, there are 810 chains in total, and the chain index varies from 1 to 810, correspondingly. To calculate the plateau level, chains with index from 1 to 405 (i.e. half of the chains) were labeled as red and the rest as blue. Since in the simulation, the distribution of red and blue chains in micelles is independent of the chain index, the distribution of red or blue chains should be random at the end of hybridization process. Using such random labeling, the plateau level then can be calculated using eq.1, i.e.

$$I_\infty = 4 < \sum_N \left[\left(\frac{N_r}{N} - \frac{1}{2} \right)^2 \frac{N}{N_{total}} \right] >$$

where N_{total} is the total number of chains, N is the micelle aggregation number, N_r is the number of red chains, and <…> denotes averaging over several configurations. As is seen from Table S1, the plateau level calculated from random labeling chains (discussed above) is practically identical to the plateau level obtained from hybridization simulations (Figure 2). We note that increasing number of chains (and correspondingly system size) would diminish the statistical deviations.

Table S1. Plateau level of the hybridization correlation function I(t) calculated from Figure 2 (main text) in comparison with the value obtained by random labeling of chains in micelles for A_2B_3 micelle solutions with interaction energy a_{AB}=50 at different oligomer concentrations.

plateau / φ	from Figure 2	from random labeling
0.02	0.10	0.10
0.03	0.07	0.08
0.04	0.06	0.06
0.05	0.05	0.05

2. Unimer insertion correlation function for A_2B_3 micelle solutions.

To calculate the chain insertion correlation function, all unimers were marked at time t=0. When a unimer joins an aggregate and remains assembled for at least two time intervals, the chain is unmarked. The unimer insertion correlation function U(t) is calculated as:

$$U(t) = < \frac{N(t)}{N(0)} > \qquad \text{(S1)}$$

where *N(0)* is the number of unimers at *t=0* and *N(t)* is the number of labeled unimers at time t, <…> denotes averaging over different initial configurations.

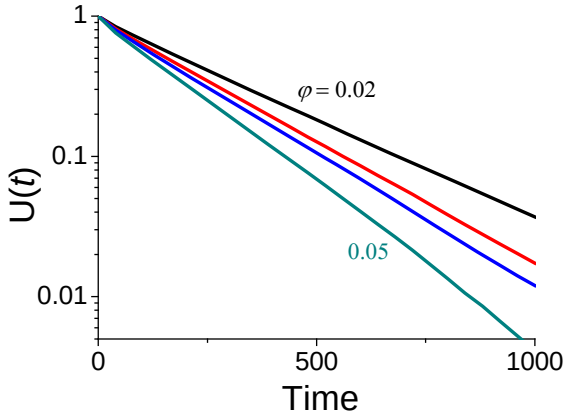

Figure S1. Unimer insertion correlation function U(t), eq. S1, for A_2B_3 micelle solutions with interaction energy a_{AB}=50 at different oligomer concentrations (φ = 0.02, 0.03, 0.04, 0.05 from top to bottom).

Figure S1 shows the unimer insertion correlation function for A_2B_3 micelle solutions (a_{AB}=50) at different oligomer concentrations. As is seen, unimer insertion follows a single-exponential decay process with a characteristic time decreasing with an increase in concentration. In Table S2, the unimer insertion relaxation times obtained by fitting the U(t) correlation function with a single-exponential decay function are given for A_2B_3 micelle solutions for different interaction energies and oligomer concentrations. As is seen, the increase in the interaction energy slows down unimer insertion while an increase in concentration speeds it up.

Table S2. Unimer insertion time $\tau_{insertion}$ obtained by a single-exponential decay fitting of unimer insertion correlation function U(t) for A_2B_3 micelle solutions with different interaction energies and oligomer concentrations.

a_{AB} / φ	*50*	*52.5*	55
0.02	280	475	832
0.03	235	395	525
0.04	212	328	459
0.05	179	273	359

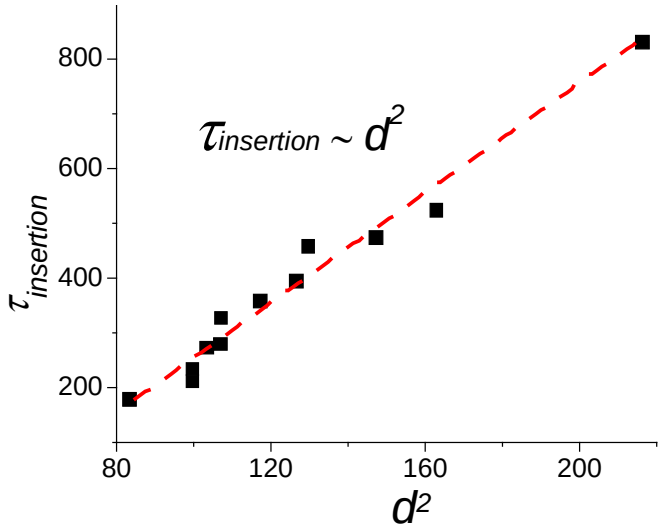

Figure S2. The unimer insertion time $\tau_{insertion}$ vs. the square of average distance d^2 between aggregates (P>1) for A_2B_3 micelle solutions with different interaction energies (a_{AB}=50, 52.5, 55), and oligomer concentrations (φ = 0.02, 0.03, 0.04, 0.05).

To understand the observed dependence of unimer insertion time $\tau_{insertion}$ on oligomer concentration and interaction energy, we estimated the average distance between two aggregates in solution: $d=(L^3/n)^{1/3}$, where L is the simulation box size and n is the average number of aggregates (counting all aggregates starting from dimers, i.e. $P>1$) in the box. In Figure S2 we plotted unimer insertion time $\tau_{insertion}$ vs. the square of the average distance between aggregates d^2. As is seen, $\tau_{insertion}$ linearly increases with d^2 in agreement with Einstein relation: $\tau \sim d^2/D$, with D being a diffusion coefficient, which is about 0.1 for a homopolymer of the same length as A_2B_3 chain. With an increase in oligomer concentration the number of aggregates in the solution increases (for a given interaction energy) and the average distance for a unimer to travel before insertion into an aggregate decreases leading to a decrease in $\tau_{insertion}$. Similarly, with an increase in the interaction energy the average aggregation number increases and the number of micelles decreases (for a given polymer concentration) resulting in an increase of the average distance for a unimer to travel to enter a micelle and therefore increasing $\tau_{insertion}$.

3. Native chain expulsion via different kinetic mechanisms.

In order to determine the contribution of different kinetic mechanisms into the process of chain expulsion we monitored the chains which escaped from a selected micelle via direct unimer expulsion, released as a part of a small aggregate ($2 \le P \le 4$) or as part of micelle fission (with an aggregation number of the smallest aggregate $P \ge 5$). For each of the kinetic processes we calculated a native chain escape correlation function F(t), eq.4, i.e.

$$F(t) = < \frac{N_{native}(0) - N_{leave}(t)}{N_{native}(0)} >$$

in which $N_{native}(0)$ was the total number of the native chains that escaped by this kinetic process. Figure S3 shows the native chain expulsion functions for A_2B_3 micelle solution (φ = 0.05, a_{AB}=50) for different kinetic mechanisms: unimer expulsion/insertion, small aggregate splitting/merging and micelle fission/fusion. As is seen, all three curves are practically indistinguishable and show single-exponential decay with nearly the same slope. Thus the characteristic times for a native chain escape by different kinetic mechanisms are very close to each other, as shown in Table 3 of the main text.

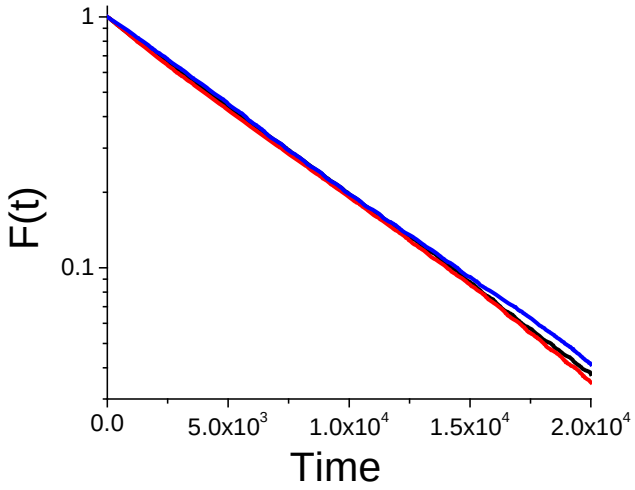

Figure S3. Native chain expulsion correlation function F(t) eq. 4 via unimer expulsion/insertion (black), small aggregate splitting/merging (red) and micelle fission/fusion (blue) for A_2B_3 micelle solution (φ = 0.05, a_{AB}=50).

4. Interaction energy effect on the contrast function.

With an increase in interaction energy a_{AB}, the exchange of chains between micelles considerably slows down and the characteristic time increases dramatically, as seen in Table S3, due to an increase in the potential barrier for chain expulsion.

Table S3. Characteristic times obtained by a single-exponential decay fitting of contrast correlation function *C(t)* for A_2B_3 micelle solutions with different interaction energies at φ =0.03.

a_{AB}	*47.5*	*50*	*52.5*	*55*
τ from *C(t)*	2703	7517	19390	44172

5. Corona-block length effect on the contrast function.

We have performed hybridization simulations and calculated the contrast correlation function using eq.2 for A_4B_x micelle solutions (a_{AB}=40) with different corona block lengths. As is seen from Figure S4, an increase in the corona block length (for a given core block) leads to more rapid chain exchange between micelles in solution, similar to the case of a_{AB}=38 (shown in Figure 4 of the main text).

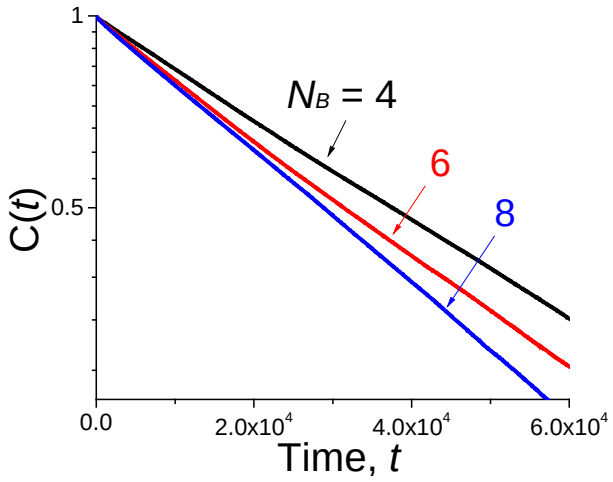

Figure S4. Contrast correlation function for A_4B_x micelle solutions with different hydrophilic block lengths (N_B=4, 6, 8) for a_{AB}=40, φ=0.05.

Table S4. Characteristic times obtained by a single-exponential decay fitting of contrast function (eq.2), native chain expulsion (eq.4) and unimer insertion (eq.S1) for A_4B_4, A_4B_6 and A_4B_8 micelle solutions with interaction energies a_{AB}=38 and a_{AB}=40 at φ=0.05.

	a_{AB}	Micelle Hybridization	Native Chain Expulsion	Unimer Insertion
A_4B_4	38	10979±409	8779±121	227
A_4B_6	38	9074±486	7740±166	229
A_4B_8	38	7372±514	6108±171	217
A_4B_4	40	54304 ±500	50336±444	466
A_4B_6	40	45497±1083	41162±493	530
A_4B_8	40	40560±393	35340±602	547

The characteristic times for chain exchange and native chain expulsion shown in Table S4 for A_4B_4, A_4B_6 and A_4B_8 micelle solutions are all decrease with an increase in corona block length indicating a quicker chain exchange process for longer corona block lengths. These characteristic times are all at least one order of magnitude higher than the unimer insertion time, as seen from Table S4, implying that chain expulsion is the rate determining step.

6. Average surface area per chain for micelles with different corona lengths.

We calculated the average interfacial surface area per chain for the micelles corresponding to the maximum of the aggregation number distribution for A_4B_x micelle solutions. The average area per chain was calculated as $4\pi<R_{core}>^2/P_{peak}$, where $<R_{core}>$ is the average core radius of the micelle with the most probable aggregation number P_{peak}. As is seen from Figure S5, the average area per chain increases with an increase in the corona-block length making it easier for a chain to escape from a micelle.

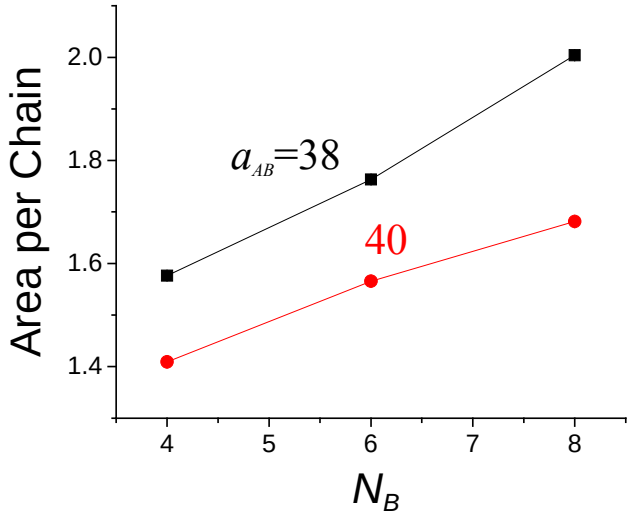

Figure S5. The average area per chain for the micelle corresponding to the maximum of the aggregation number distribution for A_4B_x micelle solutions (a_{AB}=38, 40) at oligomer concentration φ=0.05.

7. Unimer fraction for micelle solutions with different corona block lengths.

For A_4B_4 and A_4B_8 block copolymer micelle solutions with oligomer concentration φ=0.05 we calculated the fraction of unimers in the solution for different interaction energies a_{AB}. As seen from Figure S6, the fraction of unimers considerably increases as the difference in the interaction energy $\Delta a_{AB} = a_{AB} - a_{BB}$ decreases. For the same energy, the fraction of unimers is always higher for micelle solutions with longer soluble block (A_4B_8). This indicates that the longer is the soluble block length, the higher is both the critical micelle concentration and the Δa_{AB} corresponding to the onset of micelle formation, which translates into a lower critical micelle temperature.

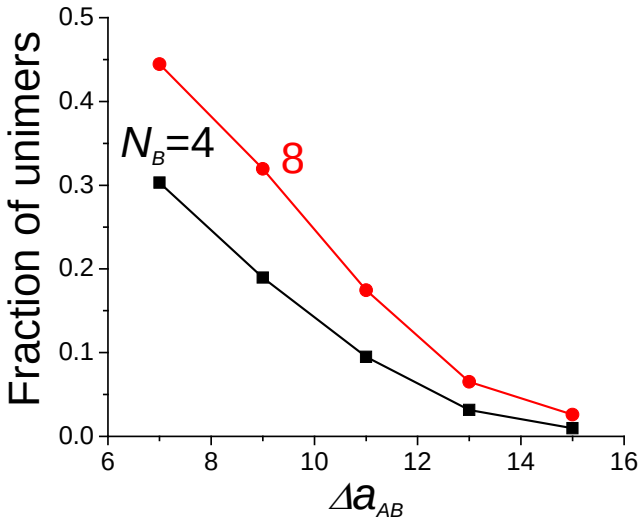

Figure S6. Fraction of unimers in A_4B_4 and A_4B_8 micelle solutions with different interaction energies $\Delta a_{AB} = a_{AB} - a_{BB}$ (a_{BB}=25) at oligomer concentration φ=0.05.

7. Corona-block length effect on chain exchange mechanisms.

To study the influence of the corona-block length on the chain exchange mechanisms, we calculated the relative frequency of different kinetic events (unimer exchange, small aggregate ($2 \le P \le 4$) expulsion/insertion and micelle fusion/fission) and the fraction of chains exchanged via the kinetic mechanisms (contribution) in A_4B_x micelle solutions with different corona block lengths. We found that as the corona-block length increases, the relative frequency and contribution of micelle fission/fusion decreases and correspondingly the frequency and contribution of unimer and small aggregate expulsion/insertion increases, as is seen from Table S5. This is to be expected, as thicker coronas make it more difficult for two micelles to come into contact to fuse.

Table S5. Relative frequency and contribution (fraction of chains exchanged) of different kinetic events for A_4B_4, A_4B_6 and A_4B_8 micelle solutions with interaction energy a_{AB}=38 at φ = 0.05.

	Event (%)			*Contribution (%)*		
	A_4B_4	A_4B_6	A_4B_8	A_4B_4	A_4B_6	A_4B_8
Unimers	60±1	64±2	65±2	29±1	37±1	40±2
Small aggregates (2≤P≤4)	34±1	32±1	32±2	39±1	44±1	47±2
Micelles (P≥5)	6±1	4±1	3±1	32±1	19±1	13±1